

Supplementary Online Material (SOM):

Cochlear morphology of Indonesian *Homo erectus* from Sangiran

Alessandro Urciuoli^{a*}, Jülide Kubat^{b,c}, Lisa Schisanowski^c, Friedemann Schrenk^{c,d}, Bernhard Zipfel^e, Mirriam Tawane^f, Lunga Bam^g, David M. Alba^a, Ottmar Kullmer^{c,d}

^a *Institut Català de Paleontologia Miquel Crusafont, Universitat Autònoma de Barcelona, Edifici ICTA-ICP, c/ Columnes s/n, Campus de la UAB, 08193 Cerdanyola del Vallès, Barcelona, Spain*

^b *CNRS UMR 8045 Babel, Université de Paris, Faculté de chirurgie dentaire, 1 rue Maurice Arnoux, 92120 Montrouge, France*

^c *Division of Palaeoanthropology, Senckenberg Research Institute and Natural History Museum Frankfurt, Frankfurt am Main, Germany*

^d *Department of Paleobiology and Environment, Institute of Ecology, Evolution, and Diversity, Goethe University Frankfurt, Frankfurt am Main, Germany*

^e *Evolutionary Studies Institute, University of the Witwatersrand, Johannesburg, South Africa*

^f *Ditsong National Museum of Natural History, Pretoria, South Africa*

^g *Department of Radiation Science, South African Nuclear Energy Corporation (Necsa), Pretoria 0001, South Africa*

*Corresponding author

E-mail address: alessandro.urciuoli@icp.cat (A. Urciuoli)

SOM Table S1

Composition of the comparative sample. Groups as used in the multivariate analyses.

Specimen	Group	Material	Provenance
F01	MH	3D model from Wimmer et al. (2019)	Extant
F02	MH	MCT scan from Wimmer et al. (2019)	Extant
F03	MH	MCT scan from Wimmer et al. (2019)	Extant
F04	MH	MCT scan from Wimmer et al. (2019)	Extant
F05	MH	MCT scan from Wimmer et al. (2019)	Extant
F06	MH	MCT scan from Wimmer et al. (2019)	Extant
F07	MH	MCT scan from Wimmer et al. (2019)	Extant
F08	MH	MCT scan from Wimmer et al. (2019)	Extant
F09	MH	MCT scan from Wimmer et al. (2019)	Extant
F11	MH	MCT scan from Wimmer et al. (2019)	Extant
Cr.3	SH	Data from Conde-Valverde et al. (2019)	Sima de los Huesos (Spain)
Cr.4	SH	Data from Conde-Valverde et al. (2019)	Sima de los Huesos (Spain)
Cr.7	SH	Data from Conde-Valverde et al. (2019)	Sima de los Huesos (Spain)
Cr.8	SH	Data from Conde-Valverde et al. (2019)	Sima de los Huesos (Spain)
Cr.12	SH	Data from Conde-Valverde et al. (2019)	Sima de los Huesos (Spain)
Cr.13	SH	Data from Conde-Valverde et al. (2019)	Sima de los Huesos (Spain)
Cr.15	SH	Data from Conde-Valverde et al. (2019)	Sima de los Huesos (Spain)
AT-421	SH	Data from Conde-Valverde et al. (2019)	Sima de los Huesos (Spain)
AT-643	SH	Data from Conde-Valverde et al. (2019)	Sima de los Huesos (Spain)
AT-1907	SH	Data from Conde-Valverde et al. (2019)	Sima de los Huesos (Spain)
La Chapelle-aux-Saints	NE	Data from Conde-Valverde et al. (2019)	La Chapelle-aux-Saints (France)
La Ferrassie 1	NE	Data from Conde-Valverde et al. (2019)	La Ferrassie (France)
La Ferrassie 2	NE	Data from Conde-Valverde et al. (2019)	La Ferrassie (France)
La Ferrassie 8	NE	Data from Conde-Valverde et al. (2019)	La Ferrassie (France)
La Quina H5	NE	Data from Conde-Valverde et al. (2019)	La Quina (France)

Kebara 1	NE	Data from Conde-Valverde et al. (2019)	Wadi Kebara (Israel)
Amud 1	NE	Data from Conde-Valverde et al. (2019)	Wadi al-Amud (Israel)
MLD 37/38	AU	MCT scan (Pal. Centre)	Makapansgat Member 4 (South Africa)
StW 53 g	AU	MCT scan (Pal. Centre)	Sterkfontein Member 4/5 (South Africa)
StW 98	AU	MCT scan (Pal. Centre)	Sterkfontein Member 4 (South Africa)
StW 151c	AU	MCT scan (Pal. Centre)	Sterkfontein Member 4 (South Africa)
StW 255	AU	MCT scan (Pal. Centre)	Sterkfontein Member 4/5 (South Africa)
StW 329	AU	MCT scan (Pal. Centre)	Sterkfontein Member 4 (South Africa)
STS 5	AU	MCT scan (Pal. Centre)	Sterkfontein Member 4 (South Africa)
StW 578	AU	MCT scan (Pal. Centre)	Jacovec Cavern (South Africa)
StW 573	AU	MCT scan (Pal. Centre)	Sterkfontein Member 2 (South Africa)
STS19	AU	MCT scan (NECSA)	Sterkfontein Member 4 (South Africa)
SK879	AU	MCT scan (Max Planck)	Swartkrans Member 1 (South Africa)
DNH22	AU	MCT scan (Pal. Centre)	Drimolen (South Africa)
SKW18	AU	MCT scan (Max Planck)	Swartkrans Member 1 (South Africa)
SK27	Early <i>Homo</i>	MCT scan (NECSA)	Swartkrans Member 1 (South Africa)
SK847	Early <i>Homo</i>	MCT scan (Max Planck)	Swartkrans Member 1 (South Africa)
Aroeira 3	Middle Pleistocene <i>Homo</i>	3D model from Conde-Valverde et al. (2018b)	Gruta da Aroeira (Portugal)

Abbreviations: AU = *Australopithecus + Paranthropus*; NE = Neanderthals; SH = Sima de los Huesos; MH = modern humans.

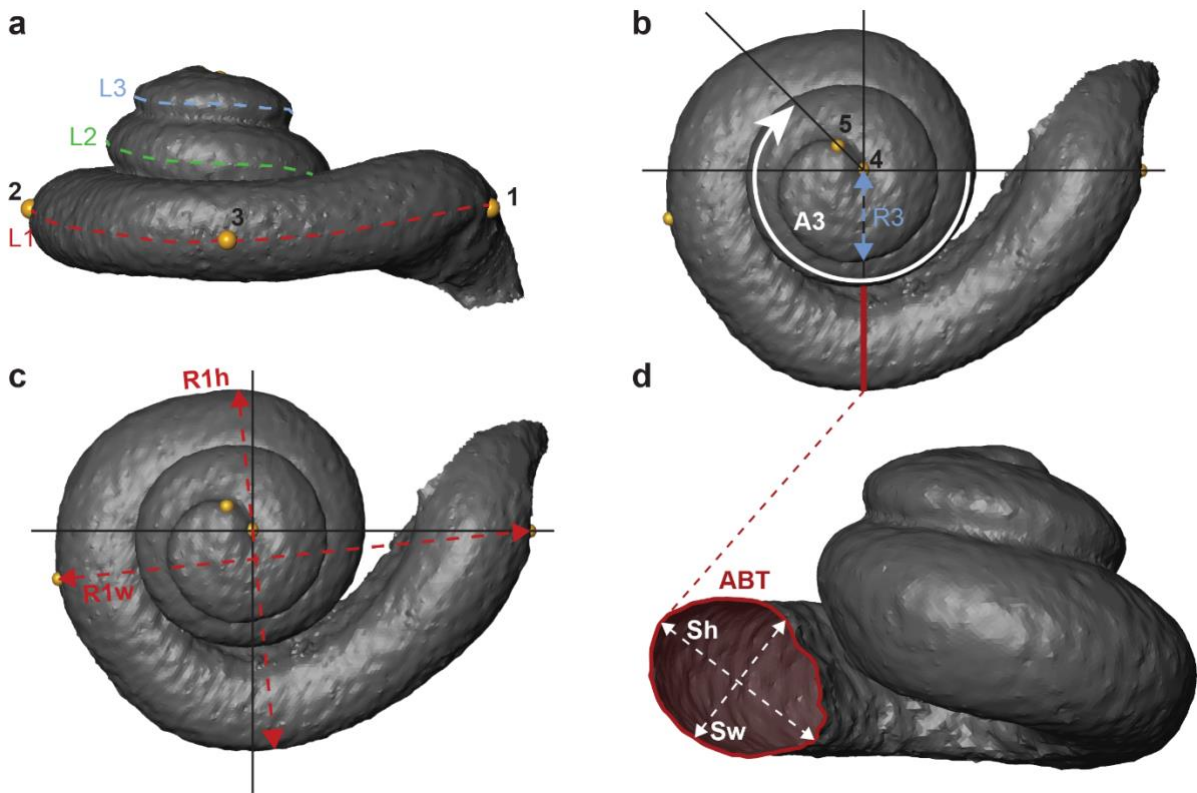
SOM Table S2

Raw data used in the regressions and multivariate analyses, as well as the aspect ratio of the cross-section (Sw/Sh).

Specimens	CL	L1	L3	Vol	Sw	Sh	R1	R3	CTh	NT	Sw/Sh
F01	40.17	21.65	6.50	79.99	1.77	2.66	3.92	1.49	2.95	2.70	0.67
F02	42.24	23.55	6.41	107.33	2.20	2.95	4.24	1.53	2.58	2.67	0.75
F03	45.47	24.74	7.26	111.26	2.03	2.72	4.48	2.18	3.01	2.58	0.75
F04	41.47	22.40	6.90	88.20	1.77	2.63	3.97	1.75	2.48	2.67	0.67
F05	39.99	23.82	4.12	94.12	2.01	2.91	4.28	1.48	2.11	2.43	0.69
F06	40.32	21.95	5.95	96.38	1.84	2.77	4.05	1.85	2.71	2.60	0.66
F07	42.23	22.15	7.61	88.97	1.75	2.33	4.07	1.93	2.41	2.70	0.75
F08	44.19	24.12	6.84	105.51	2.05	2.65	4.24	1.81	2.67	2.63	0.77
F09	43.37	23.15	7.11	101.65	1.72	2.70	4.21	1.93	2.69	2.61	0.64
F11	38.63	21.61	5.92	69.07	1.65	2.49	3.86	1.56	2.32	2.62	0.66
Cr.3	39.90	21.10	6.60	54.50	1.60	2.30	3.60	1.40	2.30	2.76	0.70
Cr.4	42.10	23.20	5.90	61.60	1.70	2.30	3.80	1.50	2.30	2.49	0.74
Cr.7	41.10	22.60	5.30	71.60	1.80	2.50	3.80	1.40	2.00	2.50	0.72
Cr.8	39.50	22.00	5.30	63.20	1.70	2.40	3.80	1.80	1.70	2.51	0.71
Cr.12	41.00	22.10	6.20	68.00	1.80	2.40	3.90	1.40	2.40	2.81	0.75
Cr.13	40.60	23.60	4.60	69.20	1.90	2.50	3.80	1.50	1.90	2.44	0.76
Cr.15	35.30	20.50	3.90	44.90	1.40	1.80	3.50	1.30	1.90	2.41	0.78
AT-421	39.10	22.80	4.60	52.60	1.70	2.40	3.70	1.30	2.20	2.53	0.71
AT-643	38.60	21.00	5.70	49.50	1.60	2.20	3.60	1.60	1.90	2.55	0.73
AT-1907	36.90	22.10	2.90	68.00	1.90	2.50	3.80	1.30	1.70	2.25	0.76

La Chapelle-aux-Saints	38.10	22.90	2.00	76.90	1.80	2.70	3.90	2.10	2.30	2.18	0.67		
La Ferrassie 1	45.00	24.90	6.80	82.80	1.90	2.90	4.10	1.80	2.80	2.59	0.66		
La Ferrassie 2	42.80	24.80	5.30	79.80	1.70	2.60	4.10	1.60	2.50	2.50	0.65		
La Ferrassie 8	36.30	21.60	3.30	54.70	1.70	2.30	3.50	1.40	1.70	2.31	0.74		
La Quina H5	43.30	26.80	2.20	102.00	2.10	2.90	4.30	1.30	2.60	2.34	0.72		
Kebara 1	42.50	24.30	4.00	83.40	1.90	2.90	4.10	1.70	2.00	2.31	0.66		
Amud 1	39.80	23.60	3.70	70.30	1.80	2.60	3.90	1.40	2.20	2.36	0.69		
MLD 37/38	40.30	22.03	4.83	94.82	1.98	2.22	3.96	1.89	2.23	2.41	0.89		
StW 53g	36.76	19.22	6.36	57.00	1.63	2.09	3.38	1.54	2.39	2.90	0.78		
StW 98	34.02	19.23	4.41	54.41	1.90	2.05	3.52	1.41	2.02	2.55	0.93		
StW 151c	31.31	17.88	3.59	36.02	1.38	1.81	3.21	1.15	1.39	2.41	0.76		
StW 255	37.19	19.74	6.25	63.40	1.69	2.37	3.63	1.69	2.08	2.67	0.71		
StW 329	33.59	18.29	5.47	47.20	1.56	1.94	3.29	1.47	1.78	2.62	0.80		
STS 5	38.49	20.89	5.69	70.22	1.96	2.36	3.67	1.46	2.03	2.69	0.83		
StW 578	36.89	20.40	5.81	61.16	1.89	2.21	3.62	1.48	1.92	2.72	0.86		
StW 573	37.00	20.87	5.50	64.51	1.70	2.41	3.77	1.21	2.77	2.77	0.71		
STS 19	33.07	18.46	4.41	40.97	1.31	1.51	3.30	1.33	1.49	2.56	0.87		
SK 879	38.48	21.37	5.30	72.17	1.97	2.57	3.80	1.53	1.96	2.60	0.77		
DNH 22	35.01	20.90	3.16	60.59	1.82	2.19	3.71	2.03	1.64	2.36	0.83		
SKW 18	35.88	21.23	3.23	58.11	1.91	2.17	3.67	1.70	1.35	2.45	0.88		
SK27	32.11	19.65	2.02	41.34	1.40	1.81	3.22	1.26	1.54	2.15	0.77		
SK847	35.73	20.70	3.52	63.74	1.75	2.39	3.72	1.69	2.06	2.33	0.73		
Aroeira 3	40.94	21.47	7.01	76.46	1.72	2.20	3.84	1.94	2.54	2.64	0.78		

Abbreviations: CL = cochlear length (mm); L1 = length of the first turn (mm); L3 = length of the third turn (mm); Vol = cochlear volume (mm^3); Sw = width of the first turn cross-section (mm); Sh = height of the first turn cross-section (mm); R1 = radius of the 1st (basal) turn (mm); R3 = radius of the 3rd (apical) turn (mm); CTh = cochlear thickness (mm); NT = number of turns.



SOM Figure S1. Three-dimensional rendering of a modern human cochlea in posterior (a), lateral (b, c) and posterior view (d) showing the measurements employed in the present study and derived from protocol established by Conde-Valverde et al. (2019). Landmarks: 1 = most lateral point of the round window; 2 = inferior-most point on the external edge of the basal turn relative to landmark 1; 3 = midpoint between landmarks 1 and 2 identified on the external edge of the basal turn; 4 = center point of the cochlea; 5 = cochlear apex. Black lines correspond to reference planes as defined in Conde-Valverde et al. (2019).

Abbreviations: L1 = first cochlear turn; L2 = second cochlear turn; L3 = third cochlear turn; A3 = angle of the third turn; R3 = radius of the third turn; R1h = height of the first turn radius; R1w = width of the first turn radius; ABT = cochlear cross-sectional area measured on the first turn; Sh = height of the first cochlear turn cross section; Sw = width of the first cochlear turn cross-section.

SOM References

- Conde-Valverde, M., Quam, R., Martínez, I., Arsuaga, J.L., Daura, J., Sanz, M., Zilhão, J., 2018. The bony labyrinth in the Aroeira 3 Middle Pleistocene cranium. *J. Hum. Evol.* 124, 105–116.
- Conde-Valverde, M., Martínez, I., Quam, R., Bonmatí, A., Lorenzo, C., Velez, A.D., Martínez-Calvo, C., Arsuaga, J.L., 2019. The cochlea of the Sima de los Huesos hominins (Sierra de Atapuerca, Spain): New insights into cochlear evolution in the genus *Homo*. *J. Hum. Evol.* 136, 102641.
- Wimmer, W., Anschuetz, L., Weder, S., Wagner, F., Delingett, H., Caversaccio, M., 2019. Human bony labyrinth dataset: Co-registered CT and micro-CT images, surface models and anatomical landmarks. *Data Brief* 27, 104782.